International Journal of
INTELLIGENT SYSTEMS AND APPLICATIONS IN ENGINEERING
ISSN:2147-6799 www.ijisae.org Original Research Paper

Power Performance Evaluation of a New MPPT Control Design Based on Synergetic Adaptive Control Optimized by PSO Algorithm for a Photovoltaic System

Kamel Hadjadj[1], Hadjira Attoui[2]

Submitted:10/03/2024 **Revised**: 25/04/2024 **Accepted**: 02/05/2024

Abstract: This study introduces an innovative approach to maximizing power point tracking (MPPT) within solar power systems, utilizing a synergetic adaptive control (SAC) mechanism. The setup includes a solar panel, a DC-DC boost converter, a resistive load, and a synergetic adaptive controller. The control system operates on a two-loop framework; the first loop identifies the peak voltage from the solar panel, providing a baseline for the second loop. This secondary loop, a sophisticated synergetic adaptive controller, maintains the system's closed-loop equilibrium by employing Lyapunov's principle. The optimization of the controller's settings is achieved through the particle swarm optimization (PSO) method. Tailored to maintain optimal power production under a range of environmental conditions, this method's effectiveness and dependability were verified through detailed mathematical simulations of a solar power system in Matlab/Simulink under varying climate scenarios. The outcomes of the simulations strongly validate the effectiveness of the proposed method.

Keywords: *Synergetic adaptive control, Maximum power point tracking, PSO algorithm, Photovoltaic system, Power transfer optimization.*

1. Introduction

In this era of rapid technological progress, humanity enjoys unparalleled comfort compared to past generations. Much of this progress stems from the ability to harness and utilize energy efficiently in daily life. However, the accelerated consumption of energy has brought about a host of problems associated with fossil energy, including high costs and environmental pollution. In response to these challenges, alternative, more cost-effective and environmentally-friendly energy sources are explored[1]. Renewable energy with its diverse array of sources, stands out as the optimal solution. Among these renewable sources, the photovoltaic generator emerges as a promising alternative. Its most notable advantages include environment sustainability and reduced maintenance costs. However, a significant drawback of photovoltaic generators is their low efficiency, which is closely tied to fluctuating weather conditions. The amount of electric power generated is inherently dependent on variables such as solar cell temperature and irradiance levels.

In recent decades, significant efforts have been made to refine various MPPT algorithms, with the goal of maximizing energy harvest from photovoltaic panels amidst fluctuating climatic conditions. This initiative has resulted in the creation of a wide array of designs, characterized by their efficiency on one side and their simplicity on the other.

Conventional techniques like are primarily adopted in MPPT strategies, such Perturbation and Observation (P&O), Hill Climbing (HC) along with Incremental Conductance (IC), represent the most commonly employed methods in MPPT[2],[3],[4] These algorithms employ a systematic flowchart approach to track the maximum power output. Renowned for their uncomplicated implementation, they offer a practical solution in MPPT applications. Despite this, their precision in consistently identifying the maximum power point (MPP) remains somewhat constrained.

Another design approach involves MPPT commands based on proportionality relationships [5],[6],[7]. This control approach relies on the proportional relationship between the characteristic parameters of PV module and optimal parameters identifying the optimum power point. A notable limitation of this technique is the power dissipation experienced during each computation of the PV module's characteristic parameters.

Artificial intelligence have also been employed for tracking the MPP, utilizing techniques, including fuzzy logic[8],[9] and artificial neural network [10],[11],[12]. These algorithms have proven to be very effective at tracking the maximum value. However, the disadvantage of these algorithms is their complexity since they involve

[1] QUERE Laboratory, Faculty of technology, University of Setif 1, 19000 Setif, Algeria
ORCID ID : 0000-0002-7600-3641
[2] QUERE Laboratory, Faculty of technology, University of Setif 1, 19000 Setif, Algeria
ORCID ID : 0000-0001-9749-3523
** Corresponding Author Email: kamel.hadjadj@univ-setif.dz*

multiple parameters associated with the system dynamics that must be accurately known.

Recently, metaheuristic optimization algorithm such as genetic algorithms (GA) [13], particle swarm optimization (PSO) [14], [15], and Artificial Bee Colony (ABC) [16], [17], which have been implemented through flowcharts tailored to each algorithm's specific characteristics. This methodology has yielded significant improvements in efficiency. However, the complexity of this approach stands out as a significant challenge.

Furthermore, a nonlinear control strategy has been proposed to address these issues. This type of control offers the advantage of ensuring system stability around the operating point, which is MPP. For instance, Sliding Mode Control (SMC)[18],[19] is known for its robustness and simplicity, however, its primary limitation lies in the chattering phenomenon. Synergetic control[20],[21],[22] is based on the same concept as sliding mode control, demonstrating simplicity in implementation and significant efficacy, especially in eliminating the chattering effects.

The Incremental Conductance algorithm has been utilized to determine the maximum power voltage, which then acts as a benchmark for an adaptive sliding mode control [23]. Although the outcomes were satisfactory, it's important to recognize that this algorithm presented a high level of complexity.

This study presents a novel MPPT design that estimates the maximum power voltage through a straightforward algorithm. The estimated maximum power voltage is subsequently utilized as a set-point in a closed-loop control system. This system integrates an innovative synergetic adaptive method, which is further optimized by employing the PSO algorithm.

To gauge the effectiveness of the suggested strategy and appraise the performance of the method, a comparative investigation was carried out in connection with a contemporary approach, known as Integral Backstepping Sliding Mode Control (IBSMC) [24].

The article's structure is as follows:

- Section 2 provides a concise overview of the photovoltaic panel model.
- In Section 3, mathematical framework governing boost DC-DC converter is elaborated upon.
- Section 4 introduces the innovative approach, particularly focusing on the development of the adaptive synergetic MPPT controller.
- In Section 5, both simulation results and analytical findings are presented, accompanied by a comparative analysis aimed at evaluating the effectiveness of the proposed strategy.
- The article concludes with a summarizing section that encapsulates the key findings.

2. PV panel modeling characteristics

In a standalone photovoltaic system, the PV generator serves as the primary and pivotal component. Its paramount importance lies in its capacity to convert sunlight into electric current. Over time, the scientific community has devised multiple models aimed at optimizing its performance. One of the traditional models is equivalent representation of PV panel, , as depicted in Figure 1 (Mars et al., 2017).

The equivalent circuit consists of a current source opposed by a diode and supplemented by a shunt resistance identified as R_s.

The equivalent model is described by the following equation:

$$I_{pv} = I_{ph} - I_d - I_{sh} \tag{1}$$

With:

$$I_{ph} = G[I_{sc} + K_i(T - T_r)] \tag{2}$$

$$I_{sh} = \frac{V_{pv} + I_{pv}R_s}{R_{sh}} \tag{3}$$

$$I_d = I_s\left[\exp\left(q\frac{V_{pv} + I_{pv}R_s}{AK_bT}\right) - 1\right] \tag{4}$$

$$I_s = I_{rr}\left(\frac{T}{T_r}\right)^3 \exp\left(\left[\frac{qE_g}{AK_b}\right] \times \left[\frac{1}{T_r} - \frac{1}{T}\right]\right) \tag{5}$$

The output current is given by:

$$I_{pv} = I_{ph} - I_s\left[\exp\left(q\frac{V_{pv} + I_{pv}R_s}{AK_bT}\right) - 1\right] - \frac{V_{pv} + I_{pv}R_s}{R_{sh}} \tag{6}$$

Where:

I_{ph} represents the photocurrent

I_{sh} is the shunt current

I_d denotes the current through the diode

I_s represents reserved saturation current

q represents electron charge

E_g stands for Energy of the band gap for silicon

K_b is Boltzmann's constant

For an ideal PV cell, a high shunt resistance R_{sh} is preferred, while the series resistance R_s should ideally be very low. The last equation (6) becomes:

$$I_{pv} = I_{ph}. - I_s\left[\exp\left(q\frac{V_{pv} + I_{pv}R_s}{AK_bT}\right) - 1\right] \tag{7}$$

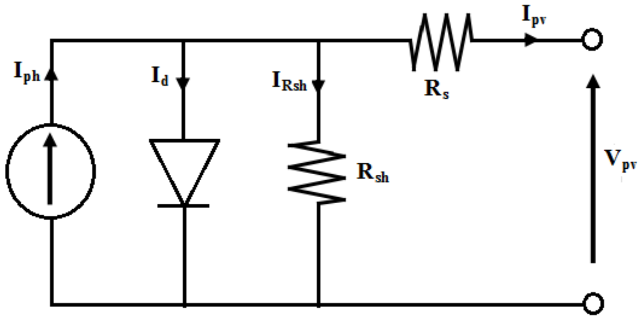

Fig 1. Equivalent Circuit of a Solar Cell

Figures 2 and 3 showcase power-voltage and current-voltage profiles of PV module across various levels of irradiance, with the temperature held constant. In a similar vein, Figures 4 and 5 reveal these profiles under varying levels of irradiance while the temperature remains unchanged. It is significant to note that (MPP) rises with a decrease in temperature or an increase in solar irradiance, highlighting PV module's nonlinear characteristics.

This nonlinearity in PV module's characteristics underscores the complexity and the challenge in efficiently extracting maximum power. The variability in the MPP with changing environmental conditions necessitates sophisticated control strategies for optimal energy harvest. As such, advanced MPPT algorithms play a crucial role in adapting to these dynamic conditions. This adaptability is not only pivotal for maximizing energy output but also for enhancing the overall reliability and lifespan of the photovoltaic system.

Table 1. Specification of PV array panel

Pmax	299.86 (W)
(Voc)	39.8 (V)
Isc	9.75 (A)
Vmp	31.9 (V)
Imp	9.4 (A)

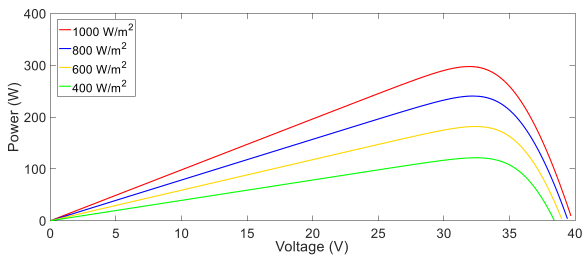

Fig 2. Power-voltage curve under different irradiances levels (T=25°C)

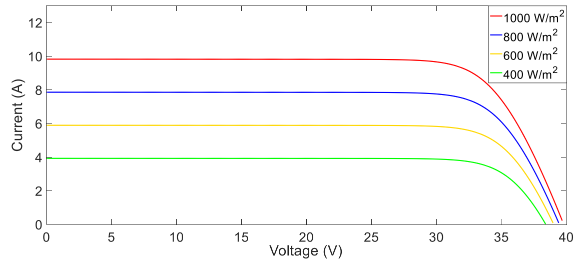

Fig 3. Current-voltage curve under different irradiances levels (T=25°C)

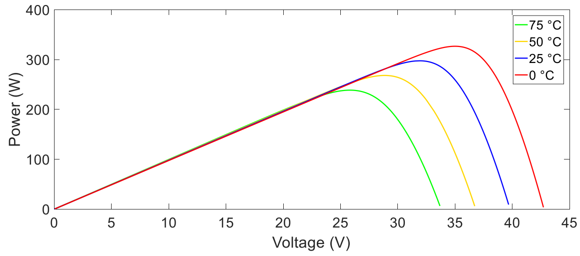

Fig 4. Power-voltage curve under different temperatures (G=1000 W/m^2)

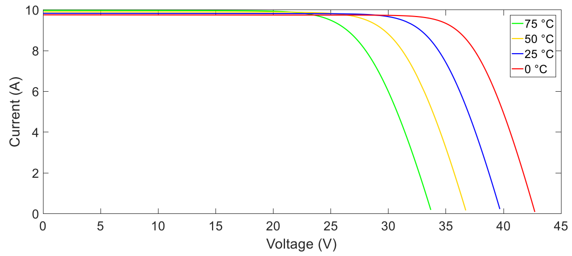

Fig 5. Current-voltage curve under different temperature (G=1000 W/m^2)

3. DC-DC boost converter

The effective use of power produced by the photovoltaic panel involves various challenges, primarily due to system's non-linear parameters, as previously discussed. To optimize power output, connecting the photovoltaic panel to the load through a DC-DC boost converter is essential. The principal objective of this controller is to guarantee a continuous maximum power output from the photovoltaic panel, even in the face of varying weather conditions. Figure 5 visually depicts the schematic diagram of the boost converter for reference.

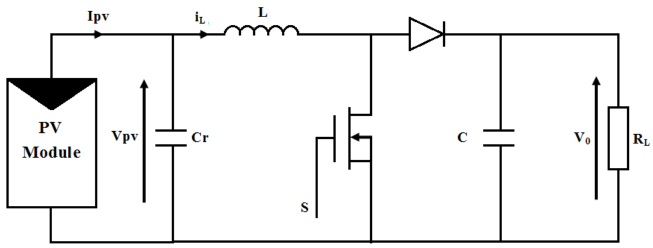

Fig 6. Simplified equivalent circuit of DC-DC boost converter linked to a PV panel

To accurately determine Pmax, MPPT controller regulates DC-DC boost converter by modulating switch S with a PWM signal. PWM signal oscillates between 0 and 1, with variations in frequency. Consequently, the operation of DC-DC boost converter is described using two states that signify the status or position of the switch S. Mathematical formulation is detailed as follows:

- First state: for switch is OFF($S = 0$), the corresponding equations are formulated as follows:

$$\frac{dV_{pv}}{dt} = \frac{I_{pv}}{C_r} - \frac{i_l}{C_r} \tag{8}$$

$$\frac{di_l}{dt} = \frac{V_{pv}}{L} - \frac{V_0}{L} \tag{9}$$

$$\frac{dV_0}{dt} = \frac{i_l}{C} - \frac{V_0}{R_L C} \tag{10}$$

- Second state: when switch is ON ($S = 1$), the equations are described as follows:

$$\frac{di_l}{dt} = \frac{V_{pv}}{L} \tag{11}$$

$$\frac{dV_0}{dt} = -\frac{V_0}{R_L C} \tag{12}$$

The comprehensive mathematical model for the nonlinear system is derived by amalgamating the two states using the state space averaging technique [20]. The model is articulated as follows:

$$\frac{di_l}{dt} = -(1-d)\frac{V_0}{L} + \frac{V_{pv}}{L} \tag{13}$$

$$\frac{dV_0}{dt} = (1-d)\frac{i_l}{C} - \frac{V_0}{R_L C} \tag{14}$$

Where the two state variables, i_l and V_0, signify current through inductor and voltage across load, respectively. V_{pv} corresponds to the voltage output from the photovoltaic module. Duty cycle of PWM signal is denoted by $d \in [0\ 1]$. L and C are inductor and capacitor components of the converter, respectively, and R_L is the resistance of the load.

4. Design of adaptive synergetic MPPT controller

The designed approach is predicated on the principle of supplying maximum voltage to the load while concurrently maintaining the power generation at its peak value.

It consists of two main parts: a maximum power voltage estimator and an adaptive synergetic controller (SAC).

- The first part comprises a maximum power voltage estimator, which calculates the voltage value corresponding to the MPP generated by the photovoltaic generator. Ensuring system stability is a prerequisite for obtaining an accurate estimation of the voltage value, and this condition is fulfilled in the second part of the design.

The secondary element consists of an Adaptive Synergetic Controller (SAC), crucial for reducing the variance between the voltage at maximum power and the load voltage V_0 to nil.

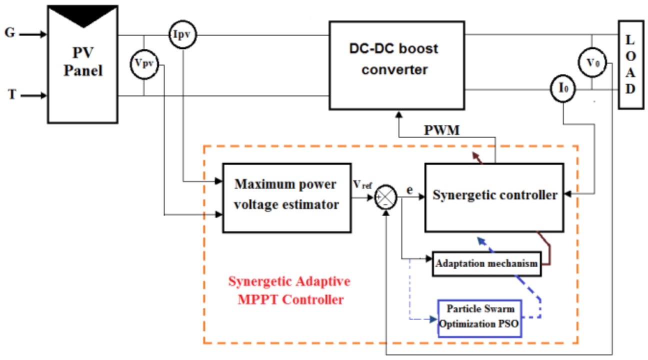

Fig 7. Bloc diagram of PV system with synergetic adaptive controller

In this segment, the adaptive synergetic controller is engineered to trace MPP. Initially, manifold Ψ was chosen as

$$\Psi = e = V_{ref} - V_0 = \frac{dP_{pv}}{dV_{pv}} = 0 \tag{15}$$

which guaranteed that the boost converter will operate as long as the power is maximum.

With $P_{pv} = V_{pv}.I_{pv}$ the manifold becomes:

$$\Psi = e = V_{ref} - V_0 = \frac{dP_{pv}}{dV_{pv}} = \frac{d(V_{pv}.I_{pv})}{dV_{pv}}$$

$$= V_{pv}\frac{dI_{pv}}{dV_{pv}} + I_{pv} \tag{16}$$

Hence, the maximum power voltage MPV is defined as:

$$V_{ref} = V_0 + V_{pv}\frac{dI_{pv}}{dV_{pv}} + I_{pv} \tag{17}$$

The intended dynamic behavior of the macro-variable is defined in the following manner:

$$\Psi + T_s\frac{d\Psi}{dt} = 0\ ;\ T_s > 0 \tag{18}$$

The projection of this dynamic on nonlinear system can be described as:

$$\frac{d\Psi}{dt} = \frac{de}{dt} = \frac{d(V_{ref} - V_0)}{dt} = \dot{V}ref - \dot{V}_0 \tag{19}$$

Upon (14), (19) can be rewritten as :

$$\frac{d\Psi}{dt} = \dot{V}ref - \frac{i_l}{C} - \frac{V_0}{R_L C} + \frac{i_l}{C}d \tag{20}$$

Substituting $\frac{d\Psi}{dt}$ from (20) into (18), (21) we obtain:

$$e + T_s\left(\dot{V}ref - \frac{i_l}{C} - \frac{V_0}{R_L C} + \frac{i_l}{C}d\right) = 0 \quad (21)$$

$$e + T_s\left(\dot{V}ref - \frac{i_l}{C} - \frac{V_0}{R_L C} + \frac{i_l}{C}d\right) = 0 \quad (22)$$

The synergetic control low given as:

$$d = 1 - \frac{\dot{V}ref.C}{i_l} - \frac{e.C}{T_s.i_l} - \frac{V_0}{R_L i_l} \quad (23)$$

We should note that the control law incorporates a load value $R_L$which can be changed as needed.

To solve this problem, we put $R_L = \frac{V_0}{I_0}$. So (23) can be

$$d = 1 - \frac{\dot{V}ref.C}{i_l} - \frac{e.C}{T_s.i_l} - \frac{I_0}{i_l} \quad (24)$$

To augment the efficacy of the proposed method, an adaptation feature was integrated. This adaptation enables Ts to dynamically adjust in response to changes in error (equation (15)), facilitating a swift response to varying dynamics, such as rapid shifts in weather conditions, so:

$$d = 1 - \frac{\dot{V}ref.C}{i_l} - \frac{\theta.e.C}{i_l} - \frac{I_0}{i_l} \quad (25)$$

With:

$$\theta = \frac{1}{T_s} \quad (26)$$

And

$$\tilde{\theta} = \theta - \hat{\theta} \quad (27)$$

Stability analysis and adaptation law

The Lyapunov function is chosen as:

$$V = \frac{1}{2}\Psi^2 + \frac{1}{2}\tilde{\theta}^T P^{-1}\tilde{\theta} \quad (28)$$

Its time derivative is

$$\dot{V} = \Psi\dot{\Psi} + \dot{\tilde{\theta}}^T P^{-1}\tilde{\theta} \quad (29)$$

Bearing in mind that $\dot{\tilde{\theta}} = -\dot{\hat{\theta}}$, then (29) can be given as:

$$\dot{V} = e\left(\dot{V}ref - \dot{V}_0\right) - \dot{\hat{\theta}}^T P^{-1}\tilde{\theta} \quad (30)$$

$$\dot{V} = e\left[\dot{V}ref - \left(\frac{i_l}{C} - \frac{\theta_2}{C}V_0 - \frac{i_l}{C}d\right)\right] - \dot{\hat{\theta}}^T P^{-1}\tilde{\theta} \quad (31)$$

Replacing d by its expression in (25), we obtain

$$\dot{\hat{\theta}}^T P^{-1}\tilde{\theta} \quad (32)$$

$$\dot{V} = e\left(\dot{V}ref - \frac{i_l}{c} + \frac{1}{c}I_0 + \frac{i_l}{c} - \dot{V}ref - e\hat{\theta} - \frac{I_0}{c}\right) - \dot{\hat{\theta}}^T P^{-1}\tilde{\theta}$$

(33)

$$\dot{V} = e\left(-e\hat{\theta}\right) - \dot{\hat{\theta}}^T P^{-1}\tilde{\theta} \quad (34)$$

Replacing (27) in (34)

$$\dot{V} = -e^2\left(\theta - \tilde{\theta}\right) - \dot{\hat{\theta}}^T P^{-1}\tilde{\theta} \quad (35)$$

$$\dot{V} = -e^2\theta + \left(e^2 - \dot{\hat{\theta}}^T P^{-1}\right)\tilde{\theta} \quad (36)$$

$\dot{V} > 0$ If $\dot{V} = -e^2\theta$
(37)

The adaptation law can be written as:

$e^2 - \dot{\hat{\theta}}^T P^{-1} = 0$ (38) Then

$$\dot{\hat{\theta}} = Pe^2 \quad (39)$$

Asymptotic stability is verified through Barbalat's lemma.

In our effort to eliminate the need for a sensor to determine i_l current value, we derive it from the current I_{pv} through (8)

$$i_l = I_{pv} - C_r\frac{dV_{pv}}{dt} \quad (40)$$

Table 2. System specifications

parameter	value
Inductor L	1 mH
Capacitor Cr	200 µF
Capacitor C	2200 µF
Load R_L	12 Ω
Adaptive gain P	0.001

5. Result and discussion

Two distinct scenarios were considered to assess its performance comprehensively, In both standardized conditions, (G= 1000 W/m^2, T = 25 °C) and under changing conditions, utilizing Matlab/Simulink simulations.

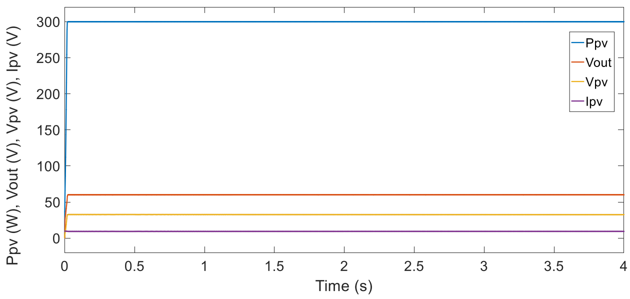

(A)

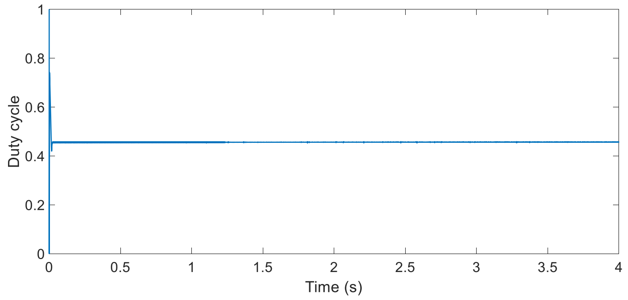

(B)

Fig 8. Simulation results conducted under standard conditions(A) Ppv, Vpv , I_{pv} , V_0 and (B) duty cycle

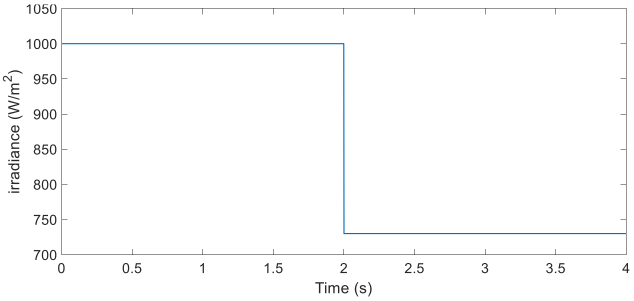

Fig 9. Solar irradiance variation

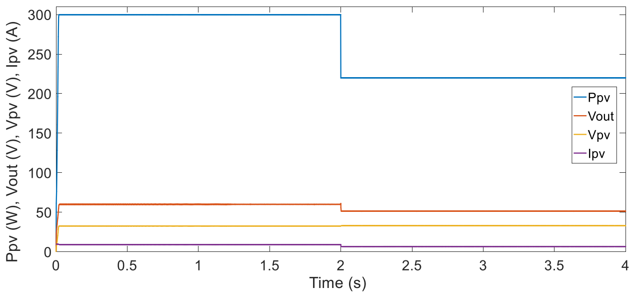

(A)

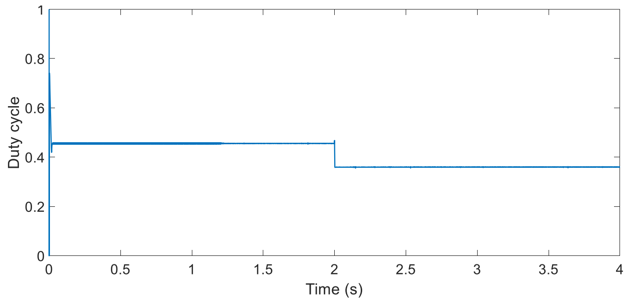

(B)

Fig 10. Simulation with stepped irradiance change

(A) Ppv, Vpv, I_{pv} , V_0 and (B) duty cycle

To assess effectiveness of the algorithm, an evaluative comparison was performed by juxtaposing its outcomes with those achieved through the Integral Backstepping Sliding Mode Control (IBSMC) approach.

The performance study involves comparing the two controllers in three criteria simultaneously: response time, power oscillation and maximum efficiency.

The latter is defined as per [25] :

$$\text{efficiency}(\eta) = \frac{\text{Experiment power}}{\text{actual power}} \times 100 \tag{41}$$

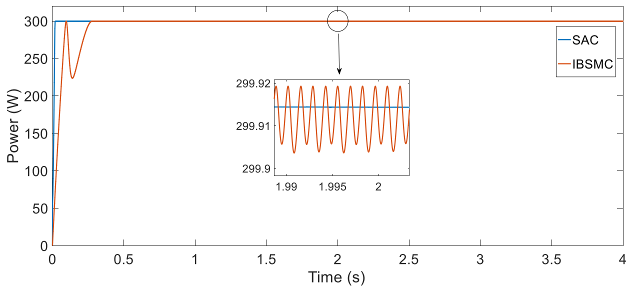

(A)

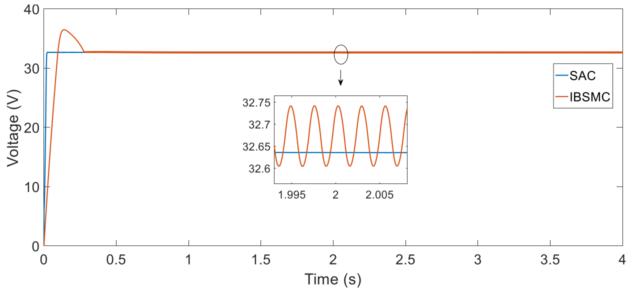

(B)

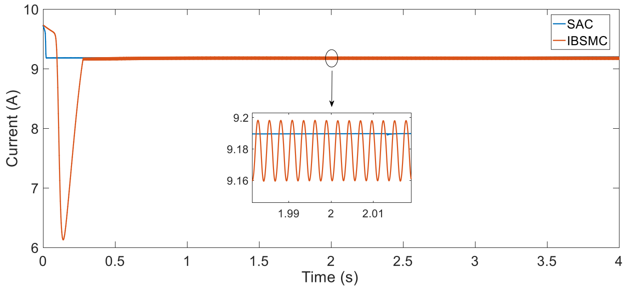

(C)

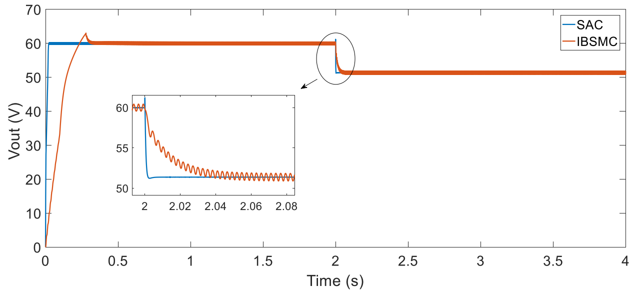

(D)

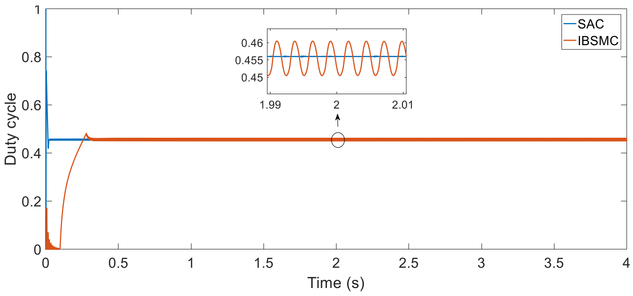

(E)

Fig 11. Simulation under standard conditions

(A) Ppv, (B)Vpv , (C) I_{pv} , (D) V_0 and (E) duty cycle

The irradiance level (Figure 9). and temperature degree (Figure 13) are abruptly altered to assess the response speed of each technique .

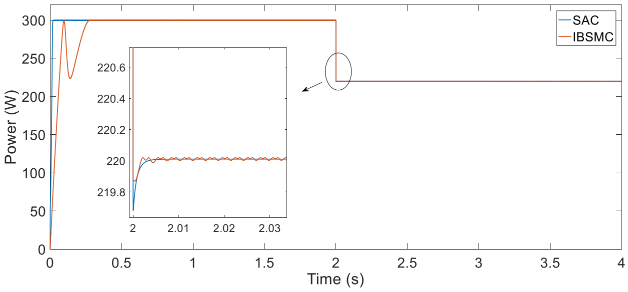

(A)

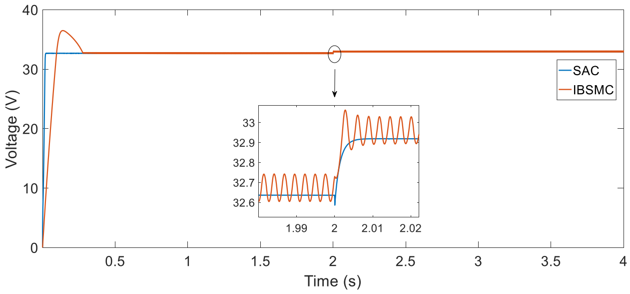

(B)

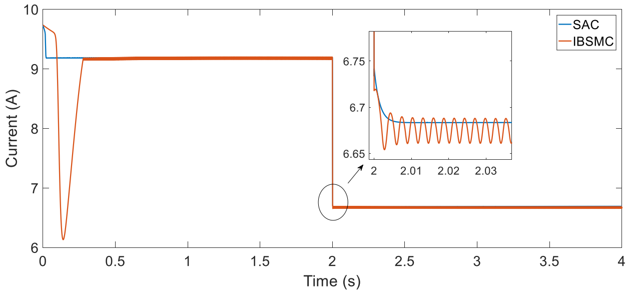

(C)

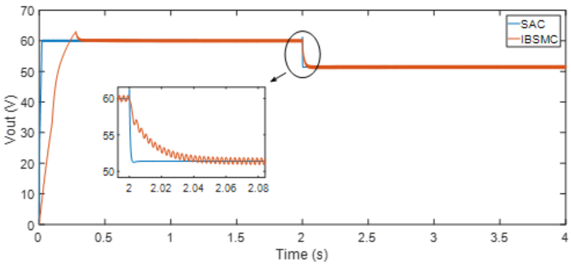

(D)

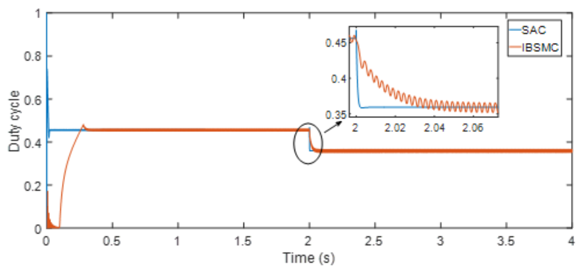

(E)

Fig 12. Simulation during rapid irradiance fluctuations

(A) Ppv, (B)Vpv, (C) I_{pv} , (D) V_0 and (E) duty cycle

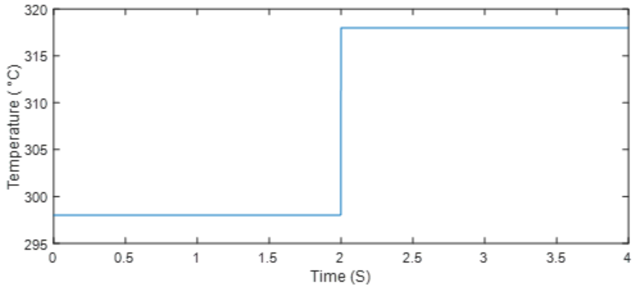

Figure 13**.** Temperature variation

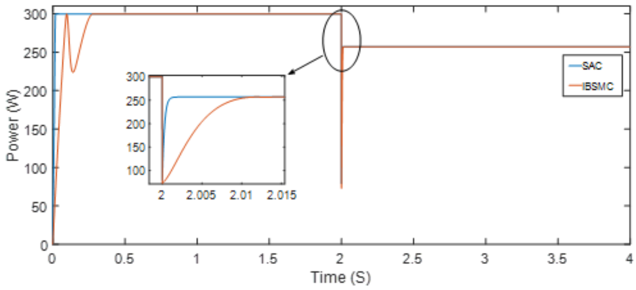

(A)

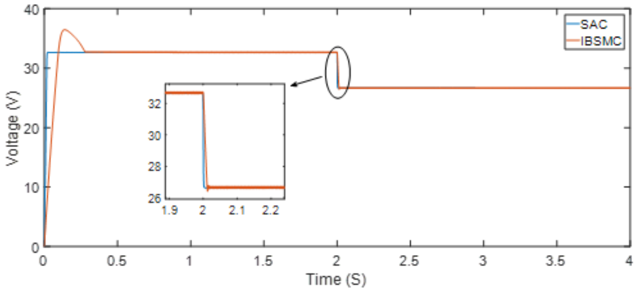

(B)

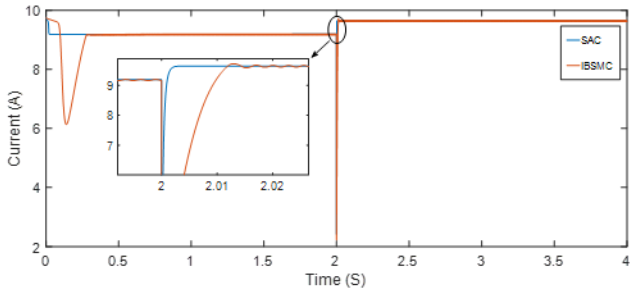

(C)

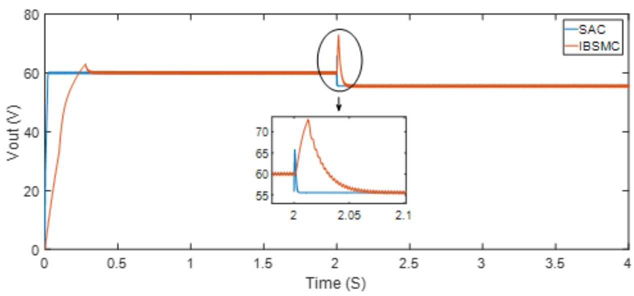

(D)

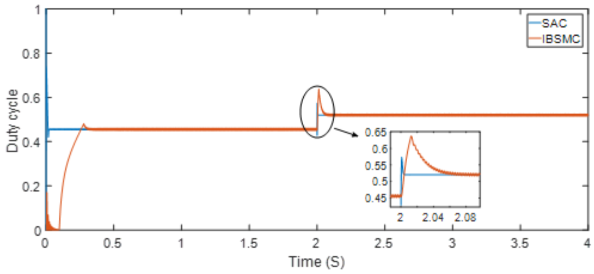

(E)

Figure 14. Simulation with step temperature change

(A) Ppv, (B)Vpv, (C) I_{pv} , (D) V_0 and (E) duty cycle

The outcomes of the simulation are:

Table 3. Performance of different controllers

MPPT Methods	Response time (ms)	Power oscillation (watt)	Max efficiency η (%)
IBSMC	27.8	0.06	98.38
SAC	2.1	0.0003	99.79

The findings underscore superior accuracy of the algorithm (SAC) in identifying the MPP, particularly in comparison to IBSMC technique. Remarkably, even amidst varying irradiance levels, this algorithm demonstrated consistent accuracy in MPP tracking, thereby emphasizing its substantial robustness against environmental fluctuations and external disturbances.

The SAC algorithm displayed notable efficiency in power conversion, maintaining a stable performance across varying irradiance levels, in stark contrast to the IBSMC. This stability is particularly crucial in settings where even minor power output fluctuations can significantly affect system effectiveness, such as in grid-connected PV systems or isolated power setups. Additionally, the SAC showcased a quicker response to environmental changes compared to the IBSMC, a key advantage in regions with rapidly shifting weather patterns, ensuring optimal power harnessing during short periods of peak solar exposure.

Furthermore, the SAC's streamlined design suggests potential benefits in terms of scalability, maintenance, and long-term reliability. Its adaptability and robust performance across diverse conditions indicate suitability for both small and large-scale PV installations. While its advancements over the IBSMC are clear, future research could focus on optimizing SAC's performance under extreme weather and integrating it with emerging technologies like energy storage systems, further enhancing the efficiency and utility of solar power systems.

6. Conclusion

This investigation introduces a synergetic adaptive control strategy, anchored in an MPPT algorithm, to effectively pinpoint MPP in a standalone photovoltaic setup under fluctuating environmental conditions, including temperature and sunlight exposure.

Matlab/Simulink simulations revealed that the synergetic adaptive strategy excelled in efficiently and precisely tracking the MPP, outperforming the IBSMC algorithm in both speed and effectiveness. Moreover, this algorithm is comparatively simpler than many contemporary algorithms, including IBSMC. The proposed method also demonstrated significant robustness and high performance, even under fluctuating weather conditions.

Moreover, the simplicity of the synergetic adaptive controller design is noteworthy. This simplicity not only facilitates easier implementation and integration into existing PV systems but also potentially reduces the overall system cost. Such cost-effectiveness, combined with the demonstrated high efficiency and robustness of the system, makes it an attractive option for widespread adoption in renewable energy applications. The future implications of this study could extend to improving the economic viability and accessibility of solar energy technologies, especially in regions where energy costs and environmental concerns are paramount.

References

[1] H. M. Namaa, “Design and Simulation of Photovoltaic Modules Performance Improvement Under the Effect of Partial Shading Using MATLAB/Simulink.,” *International Journal of Intelligent Systems and Applications in Engineering*, vol. 12, no. 21s, pp. 4251–4259, 2024.

[2] P. H. Thanh, “A Reliable Tool Based on the Fuzzy Logic Control Method Applying to the DC/DC Boost Converter of Off-Grid Photovoltaic to Track the Maximum Power Point,” *International Journal of Intelligent Systems and Applications in Engineering*, vol. 11, no. 4, pp. 831–843, 2023.

[3] A. Zegaoui *et al.*, “Comparison of Two Common Maximum Power Point Trackers by Simulating of PV Generators,” *Energy Procedia*, vol. 6, pp. 678–687, 2011, doi: 10.1016/j.egypro.2011.05.077.

[4] A. Zegaoui, M. Aillerie, P. Petit, J. P. Sawicki, J. P. Charles, and A. W. Belarbi, “Dynamic behaviour of PV generator trackers under irradiation and temperature changes,” *Solar Energy*, vol. 85, no. 11, pp. 2953–2964, Nov. 2011, doi: 10.1016/j.solener.2011.08.038.

[5] B. Yu, “An improved dynamic maximum power point tracking method for PV application,” *IEICE*

Electron. Express, vol. 11, no. 2, pp. 20130941–20130941, 2014, doi: 10.1587/elex.11.20130941.

[6] M. A. S. Masoum, H. Dehbonei, and E. F. Fuchs, "Theoretical and experimental analyses of photovoltaic systems with voltageand current-based maximum power-point tracking," *IEEE Trans. On Energy Conversion*, vol. 17, no. 4, pp. 514–522, Dec. 2002, doi: 10.1109/TEC.2002.805205.

[7] "Fuzzy Logic Based Grid Integration of Photovoltaic/Wind Hybrid Power Generation | International Journal of Intelligent Systems and Applications in Engineering", Accessed: Nov. 06, 2024. [Online]. Available: https://ijisae.org/index.php/IJISAE/article/view/5778

[8] J. Kaur and A. Khosla, "Simulation Analysis of Harmonic Mitigation in Solar Photovoltaic Based Microgrid System," *International Journal of Intelligent Systems and Applications in Engineering*, vol. 12, no. 3s, pp. 649–657, 2024.

[9] N. Kumar, A. S. Siddiqui, and R. Singh, "Intelligent Controller for Mitigating Power Quality Issues in Hybrid Fuzzy Based Microgrid Applications," *International Journal of Intelligent Systems and Applications in Engineering*, vol. 11, no. 2, pp. 719–729, 2023.

[10] H. Attia, "High performance PV system based on artificial neural network MPPT with PI controller for direct current water pump applications," *IJPEDS*, vol. 10, no. 3, pp. 1329–1338, Sep. 2019, doi: 10.11591/ijpeds.v10.i3.pp1329-1338.

[11] Carlos Robles Algarín, Deimer Sevilla Hernández, and Diego Restrepo Leal, "A Low-Cost Maximum Power Point Tracking System Based on Neural Network Inverse Model Controller," *Electronics*, vol. 7, no. 1, p. 4, Jan. 2018, doi: 10.3390/electronics7010004.

[12] S. Penta, S. Venkateshwarlu, and K. N. Sujatha, "A Novel Adaptive Controller with Lyapunov Analysis for Strategy Grid Intelligent Integrated Wind Turbine Maximum Power Point Tracking System," *International Journal of Intelligent Systems and Applications in Engineering*, vol. 11, no. 9s, Art. no. 9s, Jul. 2023.

[13] S. Hadji, J.-P. Gaubert, and F. Krim, "Genetic algorithms for maximum power point tracking in photovoltaic systems," in *Proceedings of the 2011 14th European Conference on Power Electronics and Applications*, Birmingham, UK: IEEE, Aug. 2011, pp. 1–9. Accessed: Jul. 04, 2024. [Online]. Available: https://ieeexplore.ieee.org/document/6020380

[14] F. Abdulla, "Particle Swarm Optimization Algorithm for Solar PV System under Partial Shading," *ELECTROTECHNICAL REVIEW*, vol. 1, no. 10, pp. 89–92, Sep. 2021, doi: 10.15199/48.2021.10.17.

[15] M. Balamurugan, S. Narendiran, S. K. Sahoo, R. Das, and A. K. Sahoo, "Application of particle swarm optimization for maximum power point tracking in PV system," in *2016 3rd International Conference on Electrical Energy Systems (ICEES)*, Chennai, India: IEEE, Mar. 2016, pp. 35–38. doi: 10.1109/ICEES.2016.7510591.

[16] K. Sundareswaran, P. Sankar, P. S. R. Nayak, S. P. Simon, and S. Palani, "Enhanced Energy Output From a PV System Under Partial Shaded Conditions Through Artificial Bee Colony," *IEEE Trans. Sustain. Energy*, vol. 6, no. 1, pp. 198–209, Jan. 2015, doi: 10.1109/TSTE.2014.2363521.

[17] A. soufyane Benyoucef, A. Chouder, K. Kara, S. Silvestre, and O. A. sahed, "Artificial bee colony based algorithm for maximum power point tracking (MPPT) for PV systems operating under partial shaded conditions," *Applied Soft Computing*, vol. 32, pp. 38–48, Jul. 2015, doi: 10.1016/j.asoc.2015.03.047.

[18] A. Prabhakaran and A. S. Mathew, "Sliding Mode MPPT Based Control For a Solar Photovoltaic system," vol. 03, no. 06, Jun. 2016.

[19] B. K. Oubbati, M. Boutoubat, A. Rabhi, and M. Belkheiri, "Experiential Integral Backstepping Sliding Mode Controller to achieve the Maximum Power Point of a PV system," *Control Engineering Practice*, vol. 102, p. 104570, Sep. 2020, doi: 10.1016/j.conengprac.2020.104570.

[20] H. Attoui, F. Khaber, M. Melhaoui, K. Kassmi, and N. Essounbouli, "Development and experimentation of a new MPPT synergetic control for photovoltaic systems," *JOURNAL OF OPTOELECTRONICS AND ADVANCED MATERIALS*, vol. 18, no. 1–2, pp. 165–173, Jan. 2016.

[21] N. Mars, F. Grouz, N. Essounbouli, and L. Sbita, "Synergetic MPPT Controller for Photovoltaic System," *J Electr Electron Syst*, vol. 06, no. 02, 2017, doi: 10.4172/2332-0796.1000232.

[22] kamel Hadjadj, H. Attoui, and A. Djari, "Dynamic Performance Study of an MPPT Controller Using Synergetic Controller for a Photovoltaic System," in *2024 2nd International Conference on Electrical Engineering and Automatic Control (ICEEAC*, Setif, Algeria: IEEE, May 2024, p. 6. doi: 10.1109/ICEEAC61226.2024.10576505.

[23] A. Kchaou, A. Ayadi, A. Naamane, N. M'Sirdi, and Y. Koubaa, "An Adaptive Sliding Mode Control based Maximum power point tracking method for a PV stand-alone system," in *2017 6th International Conference on Systems and Control (ICSC)*, Batna, Algeria: IEEE, May 2017, pp. 69–74. doi: 10.1109/ICoSC.2017.7958702.

[24] B. K. Oubbati, M. Boutoubat, A. Rabhi, and M. Belkheiri, "Experiential Integral Backstepping Sliding Mode Controller to achieve the Maximum Power Point of a PV system," *Control Engineering Practice*, vol. 102, p. 104570, Sep. 2020, doi: 10.1016/j.conengprac.2020.104570.

[25] A. Rawat, S. K. Jha, B. Kumar, and V. Mohan, "Nonlinear fractional order PID controller for tracking maximum power in photo-voltaic system," *IFS*, vol. 38, no. 5, pp. 6703–6713, May 2020, doi: 10.3233/JIFS-179748.